GEOPHYSICS, VOL. 54, NO. 8 (AUGUST 1989); P. 952–961, 12 FIGS.

Electromagnetic sounding in the Columbia Basin, Yakima, Washington

M. J. Wilt*, H. F. Morrison*, K. H. Lee‡, and N. E. Goldstein‡

ABSTRACT

A controlled-source electromagnetic (CSEM) survey was conducted near Yakima, Washington, to map the thickness and resistivity of a thick volcanic sequence overlying a sedimentary section and to infer structure in the sediments. The survey was conducted with a frequency-domain system employing loop transmitters 400–500 m on a side and three-component SQUID magnetometer receivers separated from the loop by 1 to 5 km. Data collected along a 30 km profile orthogonal to regional strike were interpreted initially with 1-D layered models, which were then pieced together to make a geoelectric section. Induction logs in a 5000 m exploration hole at one end of the profile agree very well with the CSEM soundings made around the hole. The geoelectric section reveals a smoothly varying thickness of volcanics with a pronounced anticlinal structure approximately concordant with a surface topographic ridge. To assess the validity of inferring lateral structure from 1-D interpretations, we made scale models of an anticlinal structure and of a surface inhomogeneity and conducted CSEM measurements over the scale models. Layered-model inversions of these data show that the anticlinal structure and its location are very well determined by 1-D inversion, but its height and width are not accurately determined. CSEM sounding over the surface inhomogeneity model shows that this feature does not significantly degrade the interpretation of a deep target layer. In this setting, a geoelectric section made up from 1-D interpretations provides good qualitative measures of subsurface structure and also provides excellent starting models for detailed 2-D or 3-D modeling.

INTRODUCTION

Under a 1983 agreement between Shell Development Co. and Lawrence Berkeley Lab (LBL), a controlled-source, frequency-domain electromagnetic sounding survey (CSEM) was made in an area between Ellensburg and Yakima, Washington (Figure 1). The purpose of the survey was to map the thickness and resistivity of the Columbia River basalt volcanic sequence and to infer geologic structure from the electrical interpretation. In particular, the experiment was designed to test the feasibility of using electromagnetic (EM) sounding to map subtle structural features at the base of the Columbia River basalts. If such features are related to concealed fold-and-fault structures, then CSEM techniques might be effective for targeting structural traps for oil and gas.

EM methods are well suited to volcanic-covered areas because the soundings are more sensitive to conductive sediments than to the usually more resistive overlying volcanics. Low-porosity welded tuffs and massive flows are essentially transparent to the EM field, whereas the deeper, more conductive sedimentary layers contribute strongly to the total measured field. In a horizontally layered medium, the depth to the contact between the volcanics and sediments can be mapped quite accurately. If the contact is of varible depth, the question arises as to how to interpret the soundings to form the electrical resistivity cross-section. Surface topography and near-surface conductive features also complicate the process (Eaton and Hohmann, 1987).

A simple first step in the interpretation process is to assume that the depth to the contact is slowly varying and to piece together 1-D interpretations to form the cross-section. Hoversten (1981) showed that this approach is effective for a 2-D model of a step fault in a resistive basement. Wilt et al. (1983) showed good correlation in field results between a 2-D interpretation of a dipole-dipole resistivity survey and

Manuscript received by the Editor July 22, 1988; revised manuscript received February 3, 1989.
*Engineering Geosciences Division, 441 Hearst Mining Building, University of California at Berkeley, Berkeley, CA 94720.
‡Lawrence Berkeley Laboratory, University of California at Berkeley, Berkeley, CA 94720.

pieced-together 1-D CSEM soundings. Keller et al. (1984) showed that time-domain EM soundings from an electric dipole source provide good average layered models to great depths, but the 1-D models did not provide structural detail along profiles.

In more recent numerical modeling studies, the detectability of a 2-D upwarp in a deep conductive layer by loop and electric-dipole transmitter systems (Newman et al., 1986; Gunderson et al., 1986) was examined. The studies showed that from electric-dipole transmitter data, the structure could not be well approximated with 1-D inversions. For central loop data, on the other hand, 1-D models gave reasonable results.

In this paper, we examine the limitations of 1-D models to interpret EM sounding data taken in volcanic-covered areas. We first present results for the Yakima-Boylston EM survey as a 2-D cross-section made from pieced-together 1-D models. These results are then discussed and compared with the known geology. To test the validity of this interpretation, we compare the field results to 2-D model data obtained from a series of analog (scale) modeling experiments. In these experiments, a surface inhomogeneity and a deep basement upwarp were modeled.

GENERAL GEOLOGY

The EM survey site lies within the Columbia basin physiographic province (Figure 1). This region is known for the thick accumulations of Miocene tholeiitic flood basalt (the Columbia River basalt group or CRBG). Gravity and seismic refraction evidence indicates that the volcanic sequence is up to 6 km thick near the center of the basin and is typically 2 km thick elsewhere (Gresens and Stewart, 1981; Catchings and Mooney, 1988). Geophysical evidence suggests that the basalts filled a Tertiary basin that was formed by continental rifting and subsidence (Catchings and Mooney, 1988). Most of the basalts resulted from eruptions between 17 and 13.5 m.y. ago (McKee et al., 1977), but significant eruptions continued intermittently until 6 m.y. ago (Hooper, 1982). Miocene-Pliocene compressive stresses have produced in the survey area high-angle reverse faults and folds that are topographically related to a series of valleys and ridges trending predominantly northwest-southeast in the area of the survey.

Figure 2 is a simplified lithologic log from Shell-Yakima YM 1-33, a 5000 m wildcat drilled in 1981. The upper 1.5 km is composed of several separate flows of CRBG. Individual flow units are estimated to contain as much as 500 km^3 of material, and all have similar compositions and textures (Lefebvre, 1970). Underlying the basalts are sedimentary rocks of the Oligocene Wenatchee formation; these are chiefly mudstones and siltstones with minor sandstone beds.

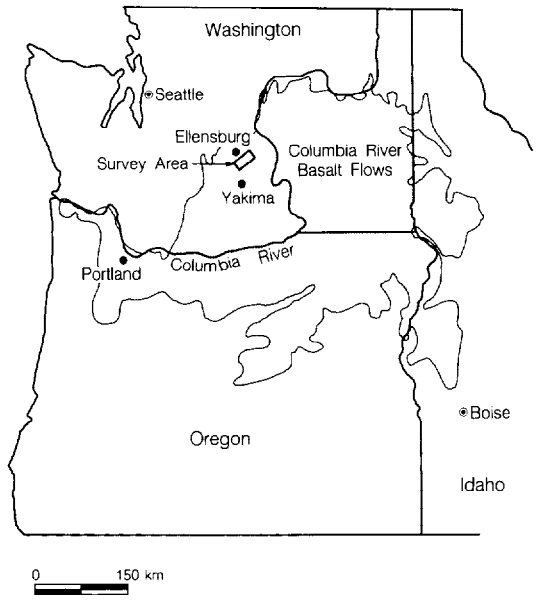

FIG. 1. Index map for the Columbia Basin physiographic province.

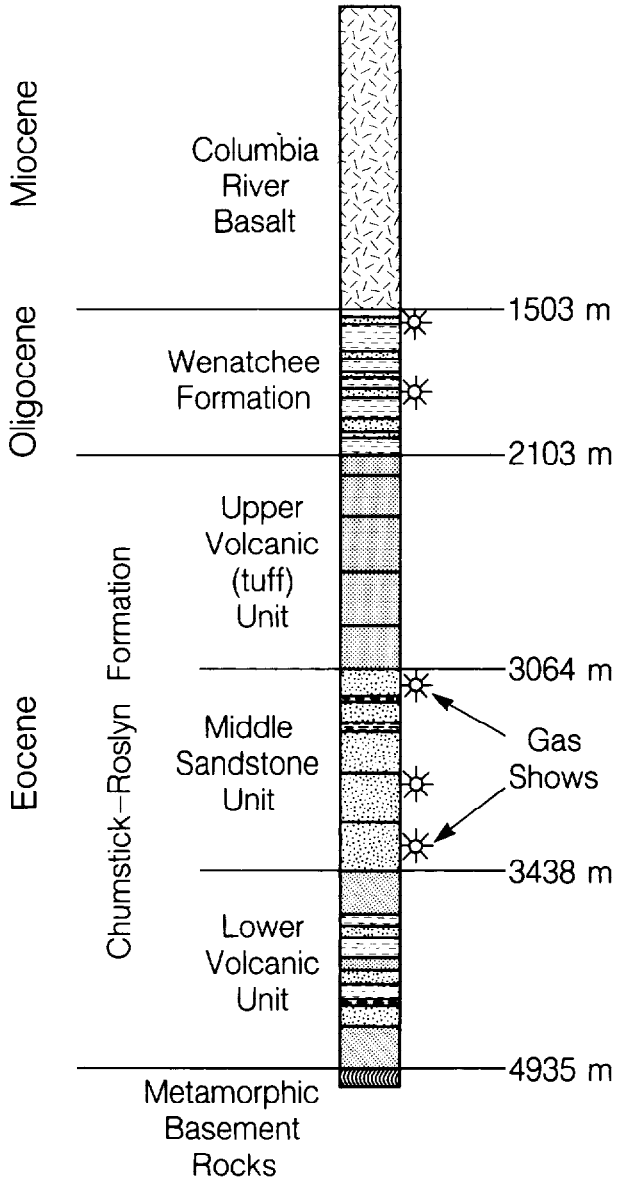

FIG. 2. Simplified geologic column from the Shell YM 1-33 well.

Although 500 m thick in YM 1-33, this formation is thought to reach a thickness of 1 km toward the center of the basin and is the main hydrocarbon target in the basin; gas shows are present in Wenatchee sandstones in YM 1-33. Underlying the Wenatchee is the Eocene Chumstick-Roslyn formation. The upper and lower members of this formation are mainly volcanic tuffs. A middle sandstone member contains thick coal beds and gave extensive gas shows in well YM 1-33.

Of principal interest in the search for petroleum in this region is the mapping of structure in the Wenatchee and Chumstick formations. Evidence from outcrops at the margin of the basin shows that the Wenatchee has broad, fairly simple structure, whereas the older Chumstick may be more complex (Curry, 1984). Although it is uncertain whether petroleum is trapped stratigraphically or by anticlines or faults, the first task is to search for structural traps. On the hypothesis that existing ridges and valleys are concordant with structures, the EM survey was designed to determine whether buried anticlines are concordant with surface ridges.

FIELD SURVEY

Locations of transmitter and receiver stations used in the EM survey are given in Figure 3. Field measurements were made with the frequency-domain EM-60 system developed at LBL and used for several years in geothermal and crustal research (Morrison et al., 1978; Wilt et al., 1983). The system is described briefly below.

The EM-60 transmitter impresses a peak current of 35–65 A, depending on the load resistance, into a horizontal-loop antenna at frequencies of 0.01–1000 Hz. The fundamental frequency of the square-wave current is controlled by one of a pair of synchronized quartz clocks. The other clock, located in the receiver-processing van, is used for the phase reference. For the Boylston CSEM survey, we used square loops 400–500 m on a side. Loop corners were surveyed with a transit and tape, and an altimeter was used to determine the inclination of the loop from the horizontal plane. For loops tilted more than about 2°, the tilt angle and tilt direction were used in computing layered models (Wilt et al., 1983).

Receiver sites were located at distances ranging from 1 to 5.5 km from the transmitters. Since the depth of penetration is a function of both frequency and transmitter-receiver separation, the closer sites generally provide a shallow depth of investigation and the more distant sites provide information to greater depths. As a general rule, the maximum depth of investigation for frequency-domain systems such as the EM-60 varies from one-half to one times the source-receiver separation. In practice, this is valid for exploration depths to several kilometers.

At each receiver site, three orthogonal components of the magnetic field were measured with SQUID magnetometers oriented to obtain vertical, radial, and tangential fields with respect to the loop. Data were taken over the frequency range 0.05–500 Hz at two sites simultaneously. Signals from a "local" magnetometer were brought to the processing van via a 30 m cable; signals from the second magnetometer, 1–3 km from the van, were sent via FM radio telemetry. Background geomagnetic fields were measured simultaneously with induction coil magnetometers for the purpose of noise cancellation (Wilt et al., 1983). Sites for background measurements were located 15 km or more from the transmitters, and these signals were also telemetered to the van, often using repeater stations. Field data were processed on site to provide initial EM parameter estimates, data quality evaluation, and apparent resistivity calculations. During 15 field days, 38 stations were occupied for an average of about 2.5/day.

Layered-model interpretations were obtained by least-squares inversion of the measured fields (Hoversten, 1981). The program, which uses a Marquardt algorithm, can use any combination of amplitude, phase, or polarization parameters as a function of frequency for the inversion. Different combinations of parameters were used for the inversions depending on the level of noise in the field components and the amount of clock drift. We tended primarily to use the polarization parameters, ellipticity, and tilt angle, since these are insensitive to clock drift and geometric errors (Smith and Ward, 1974).

The Yakima-Boylston CSEM soundings were essentially measured along a single 30 km long profile trending northeast-southwest (Figure 3). About 80 percent of the stations were located directly on the profile; the other stations were located off-line to assess the continuity of the cross-section and to obtain resistivity sections beneath the transmitter sites. The interpreted data are organized into two studies. First a comparison is made between well-log resistivity (induction log) measurements in well YM 1-33 and CSEM sounding results for stations taken around the well. Then a 30 km profile of pieced-together CSEM sounding interpretations is examined, and inferences are drawn on electrical stratigraphy and structure.

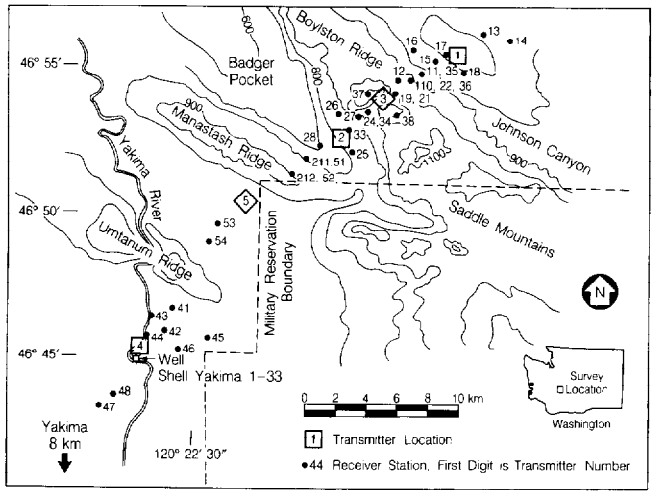

FIG. 3. Detailed survey location map for the Yakima-Boylston EM survey.

Well study

A cluster of eight CSEM soundings was made near Shell's exploration well YM 1-33 (Figure 3). Resistivity sections

obtained for these data were compared with the deep induction log from the well to evaluate the accuracy of the 1-D inversions. The soundings around the well were made from a single transmitter loop located about 300 m from the well; receiver sites were located from 1 to 4 km from the source along several azimuths.

Figure 4 shows an induction resistivity log for well YM 1-33, together with the layered resistivity sections derived at stations BP41, BP45, and BP47, three high-quality soundings made at different azimuths from the well. The well log was obtained by averaging the Schlumberger ILD conductivity log over 30 m intervals. In general, there is an excellent agreement between the well-log resistivity and the resistivity sections obtained from CSEM soundings.

Figures 5a and 5b show the ellipticity and tilt angle as a function of frequency for sounding BP41, which is located about 3 km from the loop source near well YM 1-33. The data are fit to a three-layer model of Figure 5c; error bars on the data are 75 percent confidence limits. The sounding spans three decades of frequency (0.1 Hz to 100.0 Hz), which is typical for soundings 2–4 km from the source. Closer to the source, data may be collected to frequencies as high as 1000 Hz; farther from the transmitter, soundings are measured down to 0.05 Hz.

The well data and CSEM soundings in Figure 4 show three distinct units: a high-resistivity unit extending from the surface to a depth of about 1 km, a layer of intermediate resistivity to about 1.5 km, and a deeper, low-resistivity section to more than 4.5 km. The uppermost unit consists of high-resistivity (500 ohm-m) basalt flows separated by minor sedimentary interbeds (5 ohm-m). The CSEM interpretation

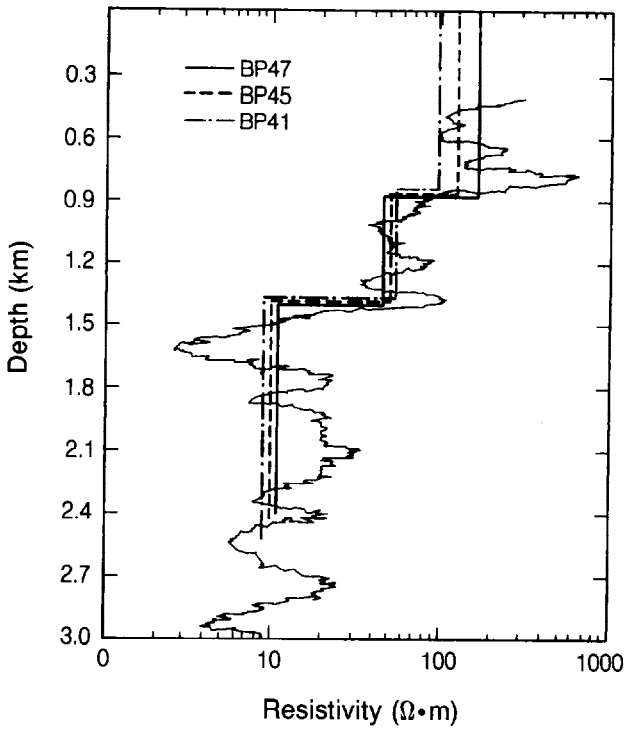

FIG. 4. Comparison of the smoothed EM induction well log from well YM 1-33 and layered-model inversions for soundings BP41, BP45, and BP47, all taken near the well.

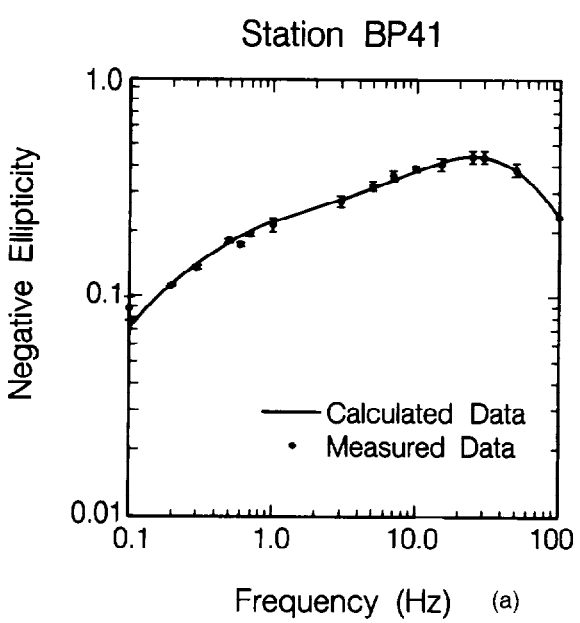

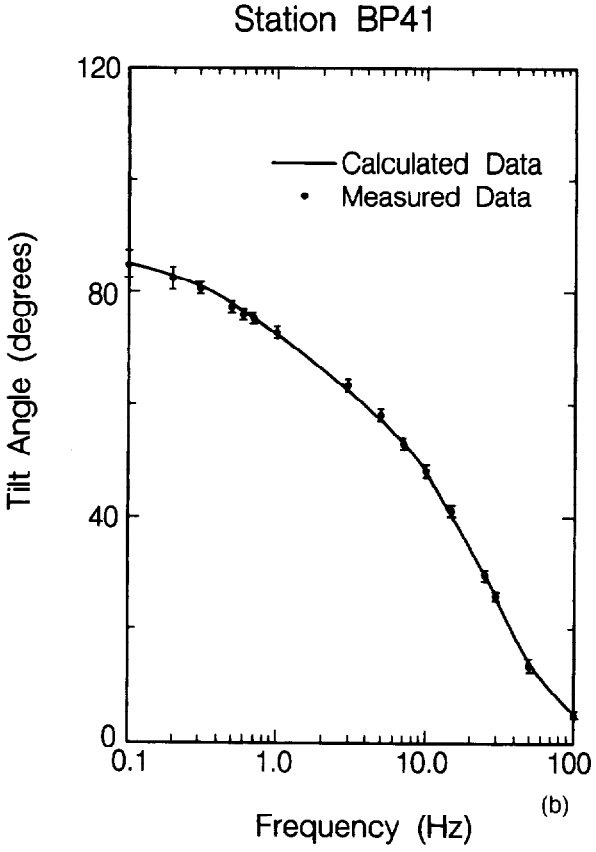

Layer	Resistivity (OHM–M)	Thickness (M)
1	99.09 ± 2.0	842.5 ± 59.0
2	65.52 ± 46.0	573.6 ± 48.0
3	8.714 ± 0.5	∞

(c)

FIG. 5. Ellipticity (a) and tilt angle (b) as a function of frequency for sounding BP41. Field data were fit to the three-layer model of (c).

accurately locates the base of this upper unit but underestimates the resistivity somewhat. The intermediate zone (1–1.5 km) is also predominantly basaltic but with many more low-resistivity sedimentary intervals, which account for the lower overall resistivity. The CSEM interpretation accurately determines the average resistivity and thickness of this unit. Below 1.5 km, the well encounters a low-resistivity sedimentary section to total depth. The resistivity of this unit is also variable, ranging from 2 ohm-m to more than 50 ohm-m; deeper sections tend to be more resistive. The CSEM interpreted resistivity ranges from 4 to 10 ohm-m: the closer-spaced soundings give the lower values; and the more distant soundings give the higher values. This interpretation is also consistent with well-log measurements, since the more distant soundings penetrate to greater depths. Our CSEM soundings did not determine the thickness of the sedimentary section in this area; but since the well log indicates that it extends to a depth of almost 5 km, this is not surprising.

Profile A-A′

An interpreted resistivity-versus-depth cross-section for profile A-A′ is shown in Figure 6. The section was constructed using a plotting convention in which the layered-model parameters for each station are plotted at a point halfway between source and receiver. The error bars on the layer boundaries are 75 percent confidence limits as indicated by the layered-model inversion statistics.

At the bottom of the cross-section we plot the magnitude of the ratio of the tangential field to the radial field $|H_\theta|/|H_R|$ at 5 Hz. This parameter, which we designate as T_h, serves as a crude indicator of the effect of 3-D complexities (e.g., surficial inhomogeneities) on the data. For a layered earth, the tangential field is zero; and the radial field is a purely secondary (induced) field. The ratio of these fields, therefore, indicates a departure from 1-D earth conditions. Anomalously high values of T_h may indicate current channeling due to surficial conductive inhomogeneities or large-scale structure. At 5 Hz the secondary fields are relatively large and the depth of penetration is typically less than 1 km, so that T_h reflects the presence of 2-D and 3-D surficial inhomogeneities more than sensor misorientation or deeper structures. We have found empirically that for T_h values less than 0.2, the inversion results are not significantly affected; for T_h greater than 0.3, the inversion results are suspect.

In general, the cross-section shows a remarkable consistency from sounding to sounding and a pattern of smoothly varying structure. The CSEM soundings indicate the following layers: (1) an intermittent low-resistivity surface layer 0–150 m thick, (2) a high-resistivity second layer 1.2–2.0 km thick that may be locally subdivided into two units, and (3) a low-resistivity third layer at least 1.5 km thick. Several of the large-offset soundings indicate a deeper, high-resistivity basal layer of undetermined thickness, but this layer is poorly resolved.

The low-resistivity surface layer is present only in Badger Pocket and near Johnson Canyon; it is thickest in Badger Pocket. The resistivity varies between 15 and 80 ohm-m, which is a typical range of values for recent alluvial and lacustrine deposits. This layer is important for two reasons. First, it helps establish the position of the top of the volcanic layer, which is necessary to determine its true thickness; this is crucial in understanding the regional structure. Second, it has a significant impact on CSEM soundings because of its high conductivity; it must be included in soundings for an accurate determination of the deeper parameters.

The high-resistivity second ("volcanic") layer is up to 2 km thick and varies in resistivity along the profile from 50 ohm-m to more than 300 ohm-m, although it averages about 200 ohm-m. This layer is believed to be the CRBG, and variations in resistivity are probably indicative of the relative contribution of sedimentary and tuffaceous interbeds in the section. The layer may be subdivided into two layers at the western end of the profile, but for soundings east of

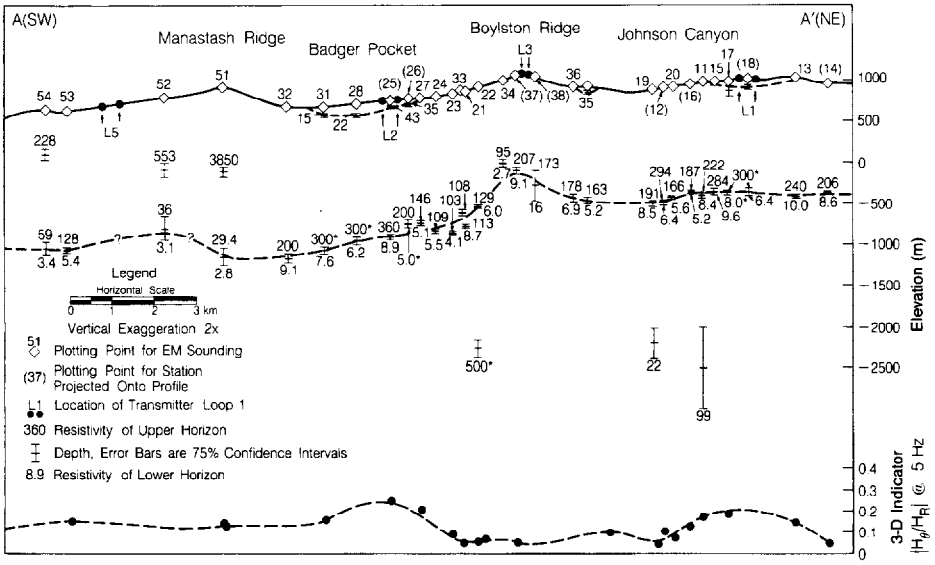

FIG. 6. Profile of pieced-together layered-model inversions for profile A-A′.

Manastash ridge, the CSEM inversions resolve only one layer. The resistivity is lowest near the Yakima River, where well YM 1-33 penetrates numerous interbeds in the CRBG. At the eastern edge of Badger Pocket, the resistivity of this layer is also fairly low (<100 ohm-m). This may also be indicative of sedimentary interbeds, but nearby soundings show a resistivity of 200–300 ohm-m, which suggests few interbeds. The low resistivity may instead reflect a distortion due to the thin, discontinous surface layer in Badger Pocket. The T_h parameter shows a maximum in this area, which probably indicates some current channeling within the conductive surface layer. The highest resistivities of the second layer are associated with Manastash and Boylston ridges.

For the third (sedimentary) layer, the resistivity ranges from 2 to 10 ohm-m;the higher values are associated with the larger offset soundings. No distinct layering was detected; hence, the resistivity increase is probably gradational, as it was in the logs for well Yakima 1-33. The thickness of this layer is not resolved by CSEM measurements, but larger offset soundings suggest that it is at least 2 km thick; it is 3 km thick in well YM 1-33.

In general, the electrical cross-section of Figure 6 indicates smoothly varying structure. The configuration of the volcanic and underlying sedimentary units (the V-S contact) seems more or less concordant with topography. Both the land surface and the V-S contact seem to dip at a shallow angle from northeast to southwest.

The most pronounced feature is an asymmetric anticlinal upwarp in the V-S contact beneath Boylston Ridge. Because the surface topography has a concordant upwarp, it appears that Boylston Ridge represents the surface expression of a simple post-CRBG fold. Note that over Manastash Ridge, the CSEM inversions do not indicate a basement upwarp. This may be due to inadequate sampling, since far fewer soundings were taken in this area due to limited access. At the eastern edge of Badger Pocket, we observe a flexure in the V-S contact, which may be an artifact of 1-D inversions near the edge of a discontinuous surface conductor. Evidence for a distortion in current flow is also given by the T_h parameter plotted at the bottom of Figure 6. This indicator jumps from less than 0.1 to more than 0.2 near the boundary.

TWO-DIMENSIONAL MODELING

Because of the unknown effects of topography and surficial conductive sediments in Badger Pocket and Johnson Canyon, there is some uncertainty about the accuracy of the 1-D inversions. Of particular interest is the upwarp in the sedimentary layer beneath Boylston Ridge. This important structure lies beneath a topographic high and is adjacent to a thick edge of conductive sediments in Badger Pocket. One test of the interpretation is to model the surface conductive feature and the 2-D upwarp in the sediments and compare these results with the field data. The relative contributions to the data of the surface structure and deep 2-D upwarp can be analyzed to determine if the pieced-together model is appropriate.

2-D modeling was done using an analog (scale) model system developed at U.C. Berkeley (Wilt and Becker, 1986). Scale-model measurements were made in the time domain with a step-response system similar in design to the UTEM system (West et al., 1984).

The modeling system, shown schematically in Figure 7, consists mostly of commercially available electronic instruments; metals are used for the modeling material. The primary field is created by a frequency synthesizer connected to a power amplifier. The output of the amplifier is connected to a hand-wound transmitter coil through a noninductive series resistor. This system is capable of generating up to 10 A for several different waveforms at frequencies from dc to 10 kHz. The receiver consists of two small coils connected to a preamplifier and then to a two-channel digital oscilloscope. Data are digitized at 10 μs intervals, averaged, and stored in the oscilloscope memory prior to processing by a desktop computer. The computer averages the data in time windows, makes calibration corrections, and prints and plots results. Measurements are made by manually moving the coils to specified positions on the model and initiating a time stack on the oscilloscope. Between 1 and 5 minutes of averaging is needed at each coil position before random error is acceptably low.

The 2-D models are shown schematically in Figure 8. The models are constructed from aluminum and lead sheets and mercury. Assuming a scale factor of 1:50 000 (1 cm = 500 m) and using resistivities for the basalt layer of 200 ohm-m and for the sedimentary layer of 6 ohm-m, we can use the scale-model relations to calculate the other model parameters (Grant and West, 1965),

$$\frac{\sigma_m \ell_m^2}{t_m} = \frac{\sigma_f \ell_f^2}{t_f},$$

where t is time in seconds, σ is the conductivity in S/m, and the subscripts m and f refer to the model and field parameters. Note that the scale models include an air layer. This layer is included to compensate for the finite height of the receiver coils above the model and the thickness of a plastic sheet upon which the measurements were made.

Because the field results were collected in the frequency domain and the scale-model data were collected in the time domain, the scale-model data must be transformed before

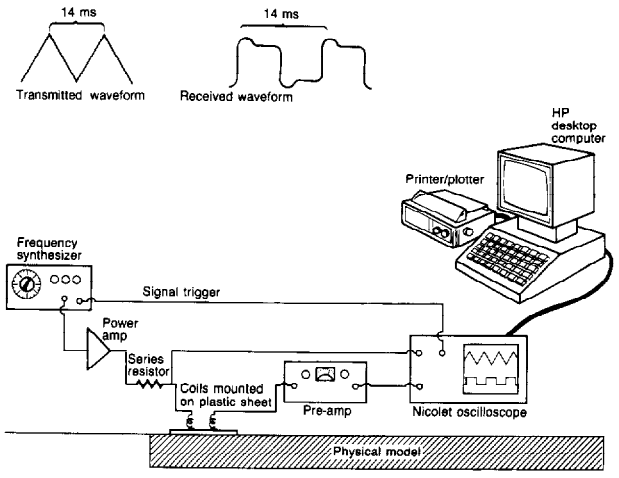

FIG. 7. Schematic drawing of the scale-model system used.

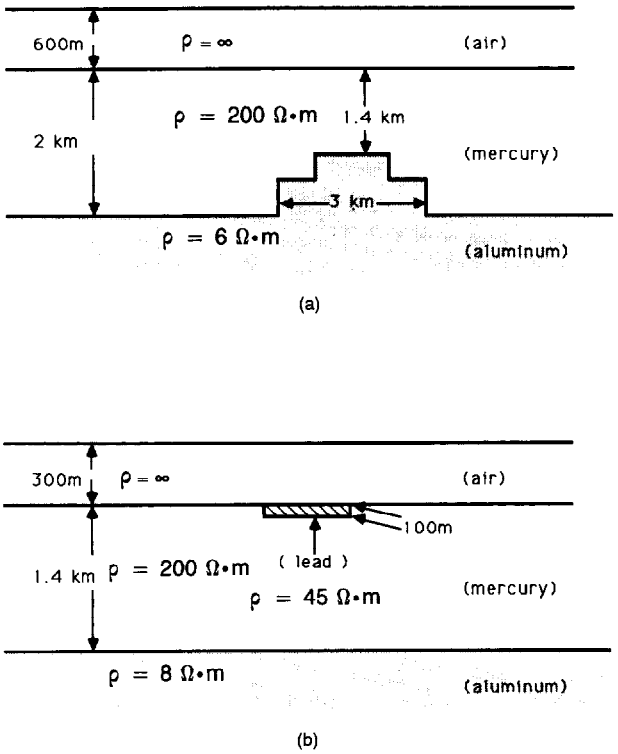

FIG. 8. 2-D models for the (a) anticline, and (b) surface inhomogeneity.

any comparison can be made. The transformation to the frequency domain was accomplished by using an interpolating cubic spline routine to resample the scale-model data at regularly spaced intervals and then performing a fast Fourier transform (FFT). The spline was needed because time-domain data are typically collected at logarithmically spaced times, whereas FFT routines require input data at equally spaced intervals. Very long transforms (typically 16 000 points) were required, since both high- and low-frequency data are needed.

RESULTS

Three types of arrays were used in the scale-model measurements: (1) a fixed-loop array, in which the transmitter remains fixed and receiver stations are at various distances; (2) a fixed-separation array, in which the transmitter-receiver separation is fixed and the pair move in tandem across the model; and (3) the central-loop array, in which the receiver is located at the center of the loop and the loop is moved across the model.

The results are presented in several ways. For the fixed-loop and fixed-separation arrays, the transformed, scale-model data are fit to 1-D models, and cross-sections are made from the pieced-together layered models. These results are then compared with the original model. For the central-loop soundings, the raw time-domain data are plotted as profiles over the structure. Since no central-loop data were taken in the field survey, layered inversions for this configuration are not presented. The time-domain profiles are useful because they provide some physical insight into the effect of this anticline; the interpreted cross-sections give an indication of the effectiveness of using 1-D models to interpret a 2-D structure.

Anticline model

The first model we consider is the anticline (Figure 8a). In this case we are attempting to map the upper surface of an upwarp in the sedimentary section beneath a surficial volcanic layer. This model is similar to the one used by Newman et al. (1986) in their numerical study.

Measurements for the fixed-separation array were made for a transmitter-receiver separation of 2 km. Both vertical and radial horizontal magnetic fields were measured at the receiver sites. Figure 9 is a plot of pieced-together 1-D inversions compared with the actual 2-D model. Scale-model data were inverted by first calculating ellipticities from the transformed data at ten frequencies from 0.5 to 100 Hz. These data were then fit to layered models with the same inversion algorithm used to fit the field data. The layer

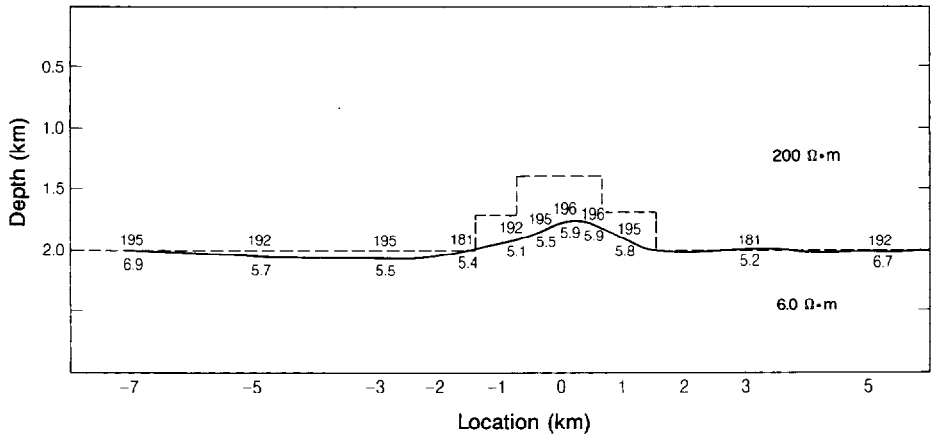

FIG. 9. Layered-model interpretation for the fixed-separation loop configuration over the anticline model. Inversion results are plotted halfway between source and receiver.

parameters are plotted midway between the transmitter and receiver.

The pieced-together layered models form a fairly good approximation to the actual model. The depth to the top of the structure is overestimated by about 15 percent; the width is underestimated by about the same amount. Considering the layered-model assumption, this result is not surprising. What is surprising, however, is that the interpreted structure is not quite symmetric. This lack of symmetry may be explained by the fact that the horizontal fields are not symmetrical over the structure (Lee and Morrison, 1985).

For the fixed-loop data, the transmitters are located at −3 km, 0, and 3 km, and receivers extend from 1.5 to 4 km from the loops on either side along the profile line (Figure 10). This arrangement is similar to the field configuration used in the Boylston-Yakima CSEM survey. Again both horizontal and vertical field components were measured, and the transformed fields were fit to layered models using 1-D inversions.

The pieced-together 1-D inversions for this model give a better approximation to the structure than the traversing fixed-separation system. For the fixed-loop system the interpreted structure appears broader than the true structure, and the resistivity of the upper layer is underestimated. One problem with the fixed-loop soundings is that the contribution from the anticline structure varies with the transmitter-receiver separation as well as with the transmitter position, so that the success in using 1-D inversions may depend on the particular array as well as the target. It is important to note that for both these separated source-receiver configurations, the midpoint plotting convention locates the anticline in the correct position. Only its amplitude and width are slightly misrepresented.

The central-loop measurements were made with a loop that scales to 1 km in diameter. This size loop is probably needlessly large for this application, but it was impractical to reduce the transmitter loop diameter and make the measurements within the loop. Figure 11a is a plot of middle- and late-time profiles of vertical magnetic field difference over the anticline structure; the fields are normalized to the magnetic field level before current shutoff. The field difference is defined as the observed field minus the field of the layered host medium away from the anticline structure. The difference anomaly is about 25 percent of the observed magnetic field, so this is, clearly, detectible structure. The data clearly show that the effect of the anticline structure is to increase the field strength in a pattern similar to the shape of the anticline. The anomaly is only evident during the middle and early late times. Outside of this time window, the response is dominated by the response of the layered host medium (Spies, 1980).

The horizontal fields for the central-loop soundings over the anticline model are also useful. Because of symmetry, the horizontal fields at the center of a loop over a 1-D earth are zero. If horizontal fields are present, they must be due to 2-D or 3-D inhomogeneities. Figure 11b shows middle- and late-time horizontal field profiles for the component measured perpendicular to the axis of the anticline. The data profiles show a typical crossover anomaly whose zero crossing occurs at the apex of the structure. Again, the anomaly is present only during the middle and early late times.

The appearance of the vertical and horizontal field data profiles (Figure 11) suggests a simple electrical analog to explain induced current flow in the anticlinal structure. One possible analog for the secondary current flow is a horizontal loop elongated in the strike direction. From the surface, this may approximate two line-current sources of opposite polarities on either side of the anticline. The fields from such a model would be similar to the observed data shown in Figure 11; the horizontal fields peak over each of the current lines, and the vertical fields form a peak halfway between the line sources.

In a recent numerical study, Newman et al. (1986) fit 1-D models to central-loop soundings made over a model very similar to the anticline model shown above. They showed that if the resistivity of the upper parts of the section can be constrained, a fairly good approximation to the true structure can be achieved by piecing together the 1-D models.

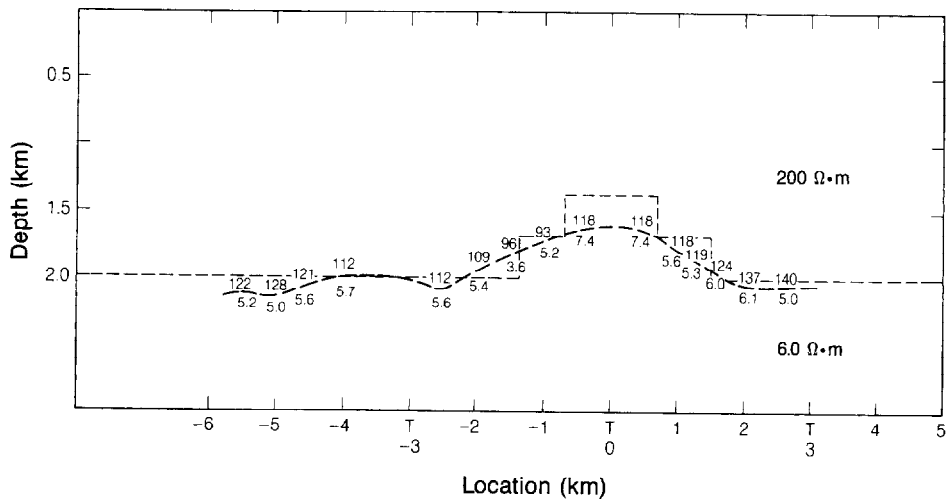

FIG. 10. Layered-model inversion results for the fixed-loop variable-offset system. Results are plotted halfway between source and receiver.

All of the arrays tested could detect the anticlinal structure, but none gave an accurate representation of the structure based on 1-D inversions. The shape and location, however, are well represented by the 1-D inversions plotted midway between the transmitter and receiver. The system providing the best estimate of the dimensions of the structure from 1-D inversions is the central-loop system. This array is sometimes difficult to use in deep sounding applications, because the transmitter loops must be quite large and only one sounding is made for each transmitter position.

Surface inhomogeneity model

The next model considered was the surface inhomogeneity shown in Figure 8b. The goal in this case was to assess the distortion caused by a thin patch of conducting overburden in a resistive surface layer. In particular, would such a surface feature cause a pieced-together 1-D interpretation to place a fictitious upwarp in a conducting basement?

The model consists of a 45 ohm-m patch 100 m thick, imbedded in a 200 ohm-m surface layer. At the base of the resistive layer is a flat-lying 6 ohm-m layer. Scale-model data were collected and processed as before. In this case, however, we used only the fixed-separation system, with a separation of 2 km, to assess the effects of the inhomogeneity.

The results of pieced-together 1-D inverisons are shown in Figure 12. In general, the surface feature does not seem to have a large effect on the results. The depth to the conductive basement is well determined except for stations at the edge of the surface conductor. For receiver stations located immediately within the inhomogeneity, the inversions slightly overestimate the depth to the conductive layer; and stations just outside of the body seem to slightly underestimate this depth. This is probably due to current channeling into the surface inhomogeneity at the expense of the more resistive host rock. A similar effect can be observed in the field data. The layered-model inversions for the stations located at the edge of Badger Pocket show a similar undershoot-overshoot effect that is manifest as a flexure in the V-S contact.

The resistivity of the top layer for stations located within the inhomogeneity is underestimated somewhat, but the distortion does not seem to cause significant errors in the determination of the thickness of this layer.

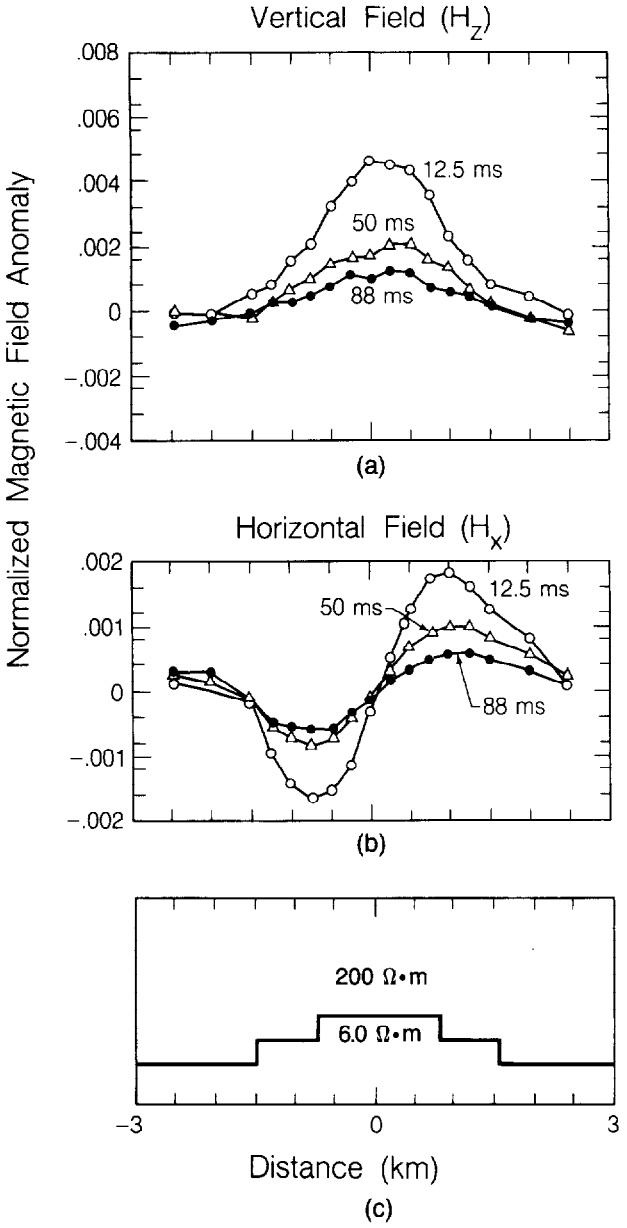

FIG. 11. Profile of magnetic field difference for the central-loop system over the anticline model. The difference is the observed field minus the field over the host medium. (a) Vertical field, (b) horizontal field, and (c) the model.

CONCLUSIONS

For mapping structure beneath surface volcanics, the EM sounding method is a very effective tool. Field data providing a depth of penetration greater than 3 km can be obtained even in rough terrain. Interpreting field data by fitting results, plotted midway between transmitter and receiver, to 1-D models and piecing these together into cross-sections provide a good indication of deeper structure. However,

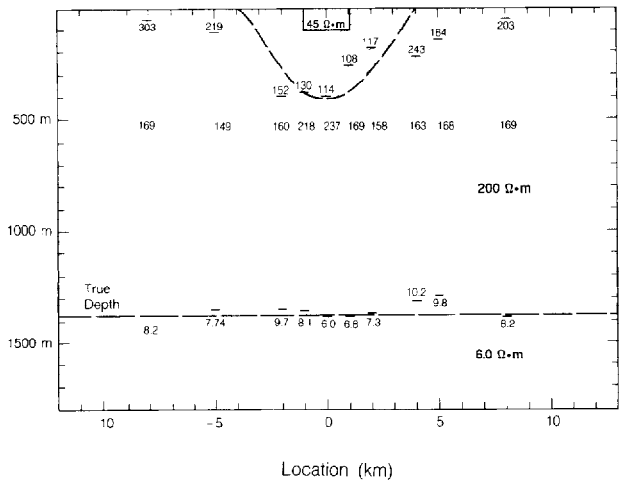

FIG. 12. Layered-model inversion results for the surface inhomogeneity model (Figure 8b).

scale-model results show that the geometry of the deeper structure is not accurately resolved. Scale models also show that thin conductive regions at the surface do not seem to have a large effect on the interpretation of deeper bodies.

ACKNOWLEDGMENTS

The authors would like to thank Shell Development Co. for supporting the field survey and, in particular, we wish to acknowledge the advice and support from Dr. Yoram Shoham. We would also like to thank LBL field crew members Ron Linnert and Ray Solhan for their capable assistance and

Hooper, P. R., 1982, The Columbia River basalts: Science, **215**, 1463–1468.

Hoversten, G. M., 1981, A comparison of time and frequency domain E. M. sounding techniques (Ph.D. thesis): Univ. of Calif., Berkeley.

Keller, G. V., Pritchard, J. I., Jacobson, J. J., and Harthill, N., 1984, Megasource time-domain electromagnetic sounding methods: Geophysics, **49**, 993–1009.

Lee, K. H., and Morrison, H. F., 1985, A numerical solution for electromagnetic scattering by a two-dimensional inhomogeneity: Geophysics, **50**, 466–472.

Lefebvre, R. H., 1970, Columbia River basalts of the Grand Coulee area, *in* Proc., 2nd Columbia River Basalt Sympos., Eastern Washington State Collge, Cheney, Washington.

McKee, E. H., Swanson, D. A., and Wright, T. L., 1977, Duration